

Research Article

Na Ta, Chutian Zhang, Hongru Ding, and Qingfeng Zhang*

Effect of tillage, slope, and rainfall on soil surface microtopography quantified by geostatistical and fractal indices during sheet erosion

<https://doi.org/10.1515/geo-2020-0036>

received April 7, 2019; accepted January 9, 2020

Abstract: Tillage and slope will influence soil surface roughness that changes during rainfall events. This study tests this effect under controlled conditions quantified by geostatistical and fractal indices. When four commonly adopted tillage practices, namely, artificial backhoe (AB), artificial digging (AD), contour tillage (CT), and linear slope (CK), were prepared on soil surfaces at $2 \times 1 \times 0.5$ m soil pans at 5° , 10° , or 20° slope gradients, artificial rainfall with an intensity of 60 or 90 mm h^{-1} was applied to it. Measurements of the difference in elevation points of the surface profiles were taken before rainfall and after rainfall events for sheet erosion. Tillage practices had a relationship with fractal indices that the surface treated with CT exhibited the biggest fractal dimension D value, followed by the surfaces AD, AB, and CK. Surfaces under a stronger rainfall tended to have a greater D value. Tillage treatments affected anisotropy differently and the surface CT had the strongest effect on anisotropy, followed by the surfaces AD, AB, and CK. A steeper surface would have less effect on anisotropy. Since the surface CT had the strongest effect on spatial variability or the weakest spatial autocorrelation, it had the smallest effect on runoff and sediment yield. Therefore, tillage CT could make a better tillage practice of conserving water and soil. Simultaneously, changes in semivariogram and fractal parameters for surface roughness were examined and evaluated. Fractal parameter – crossover length l – is more sensitive than fractal dimension D to rainfall action to describe vertical differences in soil surface roughness evolution.

Keywords: geostatistical analysis, DEMS, soil erosion process, spatial distribution, surface roughness

1 Introduction

Soil erosion is a major environmental problem worldwide [1,2], which mainly occurs on the tilled sloping surface and causes serious ecological deterioration in highly susceptible regions such as the Chinese Loess Plateau. Compared with the geomorphology, microtopography means the undulating surface configuration with fewer changes in relative elevation (usually not more than 5–25 cm) over a relatively small area under the combined effects of surface covers, rainfall, and tillage treatment [3]. During the erosion process, the elevation of the microtopographic surface varies and the surface roughness changes, which will affect the hydrological processes temporally and spatially (such as splash erosion, sheet erosion, and gully erosion).

Sheet erosion is an initial stage occurring in runoff erosion and also the initial form of erosive surface alteration [4]. In the sheet erosion stage, the top layer of surface soil is uniformly removed by the forces of raindrops and overland flows. The effect of water droplets striking the soil surface can increase the sheet flow turbulence, thereby increasing the sediment transport capacity and the severity of erosion [5]. Therefore, the relative elevation of each soil surface point varies, and the soil surface may be dotted with many small puddles. Spatial distribution of soil surface points is important for understanding the overland flow generation and the surface runoff [6]. Many precious studies have proved that tillage methods and slope gradients can influence the spatial distribution of runoff and the susceptibility of surface soil to erosion [7–9]. Although how to quantify the processes and the mechanism through the change in surface roughness, especially in a single erosion stage, i.e., sheet erosion, is still unclear, it has practical significance for understanding the relationship between microtopography and erosion and weighing tillage practice options.

* **Corresponding author: Qingfeng Zhang**, College of Natural Resources and Environment, Northwest A&F University in Yangling, Shaanxi, China, e-mail: zhqf@nwsuaf.edu.cn

Na Ta, Chutian Zhang: College of Natural Resources and Environment, Northwest A&F University in Yangling, Shaanxi, China, e-mail: tana0214@163.com, zhangchutian@nwfau.edu.cn

Hongru Ding: College of Life Science, Northwest A&F University in Yangling, Shaanxi, China, e-mail: dinghongru@nwsuaf.edu.cn

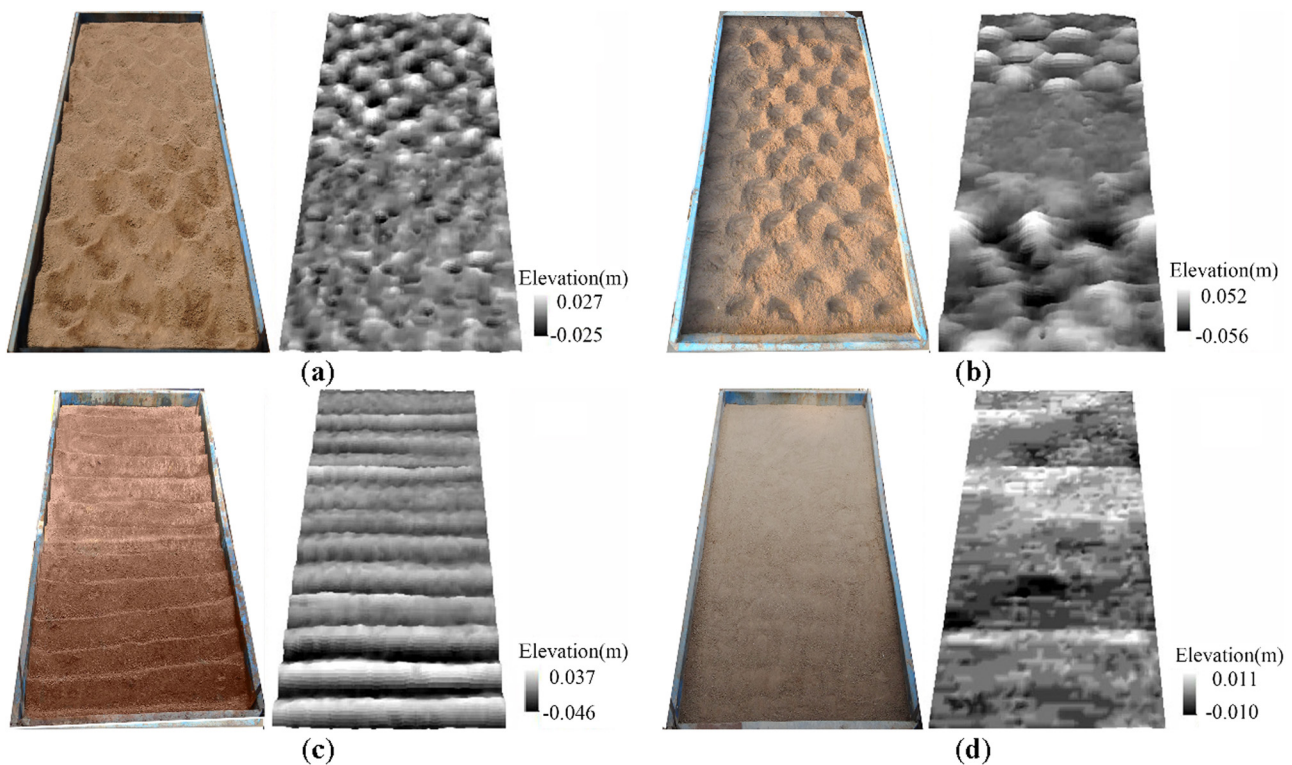


Figure 1: Traditional tillage treatments with surface difference in elevations before and after rainfall events: (a) artificial backhoe (AB); (b) artificial digging (AD); (c) contour tillage (CT) and (d) linear slope (CK).

The term “spatial heterogeneity” or “spatial variability” was widely used to present uneven spatial distribution of the relative elevation of each soil surface point [10,11], based on digital elevation model (DEM) datasets [12]. The spatiotemporal variability of the microtopographic surfaces was systematically studied [3,13–15] through all the erosion stages, and the surface relative elevation during the evolution was found to be closely related to rainfall intensity, slope gradient, and tillage practices. For specific erosion stages, i.e., sheet erosion, the effects of rain intensity and slope are still not well illustrated. So, the aim of this study is to characterize the change in roughness of microtopographic surfaces in the process of sheet erosion.

2 Materials and methods

2.1 Experimental procedure

2.1.1 Studied soil

The soil used in this study was “loutu” soil with 2.82% sand, 55.74% silt, 41.44% clay, and 16.66 g kg^{-1} soil

organic matter. This kind of grey-brown, loose, and silty sand aggregate can be classified as an Earth-cumuli-Orthic Anthrosol (USDA Taxonomy) or Anthrosols (AT) [16]. The soil was collected from the top 20 cm layer on the farmland ($108^{\circ}03'29''\text{E}$, $34^{\circ}18'24''\text{N}$) in Yangling of Shaanxi province, which is located at the southern edge of the Chinese Loess Plateau.

2.1.2 Experimental setup

In order to simulate field slopes in the natural environment, the soil sample was air dried, gently crushed, sieved through a 10 mm sieve, and packed into $200 \times 100 \text{ cm}$ slope-adjustable soil tanks to a depth of 100 cm, which was evenly divided into ten layers. The amount of soil in each layer was kept as constant as possible to maintain a target bulk density (1.30 g cm^{-3}) and a uniform spatial distribution of soil aggregates among layers [17]. The repacked soil was wetted before each experiment day, and the moisture content by mass was gravimetrically adjusted to 10 g/100 g prior to the rain simulation tests. Subsequently, three typical inclined planes of 5° , 10° , and 20° were set. Farmers experienced in the given tillage methods were employed to

implement the four commonly practiced tillage treatments in areas of Chinese Loess Plateau: (1) artificial backhoe (AB), which was traditional cultivation using a hoe to dig to depths of 4–5 cm; (2) artificial digging (AD), which was tillage using a pickaxe to dig to depths of 5–8 cm with an inter-row space of 20–25 cm; (3) contour tillage (CT), which was horizontal tillage in the direction which is perpendicular to the slope with a ridge height of 15–25 cm; and (4) linear slope (CK), which was a raked, relatively smooth slope (Figure 1). Each treatment was conducted three times.

A portable, computer-controlled, variable intensity rainfall simulator with a sprinkler system [18] was used to apply rainfall [19]. Soil erosion is strongly linked to the maximum 30-min rainfall intensity (E_{30}). In Yangling, the E_{30} value expected to occur once per 10 years or once per 30 years reaches up to 64.65 mm h^{-1} and 88.52 mm h^{-1} , respectively. Hence, the experimental rainfall intensity in this study was set to be 60 and 90 mm h^{-1} and duration to be 45 min (for 60 mm h^{-1}) or 30 min (for 90 mm h^{-1}), respectively, during the sheet erosion process. Rainfall events for 60 and 90 mm h^{-1} were conducted three times. The surface runoff sediment samples were collected every 30 s. Finally, runoff and sediment yield from each surface were measured.

A laser rangefinder was used for the automated measurement in a regularly spaced grid ($2 \times 2 \text{ cm}$) for each surface before and after the rainfall events [20]. Subsequently, these points were subjected to kriging interpolation to produce DEM data [3]. When the initial elevation of DEM before rainfall event was subtracted by the elevation of DEM after the rainfall event, the Difference in Elevations of the Microtopographic Surface (DEMS) was obtained for the study [21].

2.2 Characterization of the spatial variability

A semivariogram (SM)-based framework [14] established in our previous works was employed.

2.2.1 SM function

An SM method was used to quantify the spatial variability of the sloping surfaces [22]. The SM graph can be depicted using theoretical models such as spherical, Gaussian, exponential, or linear models. These models have the following five important parameters: (1) the structural variance C ; (2) the nugget variance C_0 ; (3) the sill ($C + C_0$);

(4) the nugget-to-sill ratio, a ratio of $C_0/(C + C_0)$; and (5) the codomain or range A .

2.2.2 Anisotropic function

In practice, the SM function $\gamma(h)$ of the regionalized variable is not only related to the distance h but also to the tillage direction [23]. Therefore, the anisotropy ratio $k(h)$ in eight directions of 0° , 25° , 50° , 75° , 100° , 125° , 150° , and 175° is used to describe the anisotropy of the surface microtopography. The $k(h)$ can be expressed as a function of division of the largest range (A_{major}) by the smallest range (A_{minor}): $k(h) = \gamma(h, \theta_1)/\gamma(h, \theta_2)$, where $\gamma(h, \theta_1)$ and $\gamma(h, \theta_2)$ is the SM at directions θ_1 and θ_2 , respectively. If $k(h)$ is equal to or close to 1, it indicates that the spatial variability is uniform in all directions, or isotropic and vice versa. A greater $k(h)$ indicates a stronger spatial variability or weak autocorrelation, while a smaller $k(h)$ indicates a weaker spatial variability or a stronger spatial autocorrelation.

2.2.3 Fractal method

Accurate description of soil surface roughness by fractal analysis relies on estimation of two commonly used fractal indices [24]: fractal dimension, D , which describes how roughness changes with scale, and crossover length, l , specifying the variance of surface roughness at a reference scale.

As the relative elevation of microtopographic surfaces exhibits a double logarithmic linear trend near the true origin [25], the fractal dimension D used to characterize the spatial variability of a microtopographic surface [26] can be given by:

$$D = 2 - m/2, \quad (1)$$

where m is the slope of the double logarithmic SM. D at different scales can be obtained according to a piecewise fitting slope.

The crossover length, l , derived from SM analysis, is a measure of the vertical variability of soil surface microtopography, which can be obtained from the log–log behavior of the expression for $\gamma(h)$ [24,27].

$$\gamma(h) = l^{1-H}h^H, \quad (2)$$

where H is the Hurst exponent ranging from 0 to 1, a measure of the degree of correlation between the surface elevations at lag distance h . As defined in [28], H may be estimated by:

$$l = \exp\left[\frac{a}{2 - 2H}\right], \quad (3)$$

where a is the intercept of the straight line of the SM as $h \rightarrow 0$. The fractal analysis parameters together with the SM parameters can be adequate for the characterization of the surface microtopography independent of the scale of the measurements.

3 Results

3.1 Overall spatial variation

3.1.1 SM model

An SM model was fitted to each of the surfaces with its parameters analyzed (Table 1). The determined coefficient is greater than 0.25, all residual sum of squares is smaller than 5.36×10^{-6} , and the coefficient for Kriging cross validations is greater than 50%; thus, these SM theoretical models can be used to simulate the elevation change in the microtopographic surfaces with a medium to strong autocorrelation. Hereinto, the Gaussian model can be widely adopted, which is well consistent with our previous works [3,13–15].

3.1.2 Variations in nugget-to-sill ratio by rainfall, slope, and tillage

The nugget-to-sill ratio of <75% (Figure 2) demonstrated that the spatial variability of the surface microtopography has medium or strong autocorrelation or dependence in the sheet erosion process. Most of the nugget-to-sill ratio was <50% except for DEMS of CT, which shows that the spatial variability of DEMS was mainly affected by geomorphologic properties and randomness, and the geomorphologic properties contributed the most. That is to say, artificial tillage measures contributed more than rainfall force in the sheet erosion stage.

Meanwhile, the nugget-to-sill ratio of DEMS for different surfaces differed greatly, when slope and rainfall varied. As the slope increased from 5° to 20° , the nugget-to-sill ratio for DEMS with the same tillage measure decreased slightly. As the rainfall intensity increased from 60 to 90 mm h^{-1} , the average nugget-to-sill ratio increased from 15.7% to 24.3%. The spatial autocorrelation of DEMS increased at a higher slope gradient and decreased at a greater rainfall

intensity. In particular, the maximum nugget-to-sill ratio was 64.9% for DEMS of surface CT under a 90 mm h^{-1} rainfall and at a 5° slope. The average nugget-to-sill ratio for DEMS of CT was the highest (44.0%). This characteristic meant that the CT surface had a relatively weaker autocorrelation and a complex spatial structure.

3.1.3 Autocorrelation range

The range A showed greater variations in DEMS with different tillage treatments (Figure 2), and it varied when three different slope gradients and the two rainfall intensities were, respectively, applied. As the slope increased from 5° to 20° , A decreased greatly; however, the average A increased from 0.23 to 0.39 m when the rainfall intensity shifted from 60 to 90 mm h^{-1} . This showed that the spatial autocorrelation decreased with decreasing slope and increased with bigger rainfall intensity. The spatial autocorrelation of surfaces CT, AD, AB, and CK was in the ascending order, as the average A was 0.88, 0.14, 0.13, and 0.10 m, respectively. Similarly, this result showed that treatment CT had the weakest effect on spatial autocorrelation.

3.1.4 Anisotropy

Figure 3 shows that the soil surfaces had anisotropic properties. The anisotropy under rainfall of 60 and 90 mm h^{-1} at slope of 5° and 25° was 1.90 and 2.04, respectively. It demonstrated that the anisotropy ratio $k(h)$ increased under a stronger rainfall.

The $k(h)$ at slope of 5° , 10° , and 20° was 2.23, 1.82, and 1.57, respectively. This result showed increasing anisotropy with decreasing slope gradient. In regard to tillage measures, the $k(h)$ under the four tillage treatments (AB, AD, CT, and CK) was 1.87, 2.01, 2.06, and 1.67, respectively. This indicated that treatment CK had the weakest effect on anisotropy, whereas the strongest anisotropy was observed for roughness of surface CT.

3.1.5 Fractal analysis

In Figure 4, the DEMS treated with different tillage methods had complex influence on fractal properties. (1) The D values at different slopes decreased in the order of D_{5° (1.88 m) > D_{10° (1.87 m) > D_{20° (1.70 m). This result showed a decrease in D on a steeper slope. (2) The D values for surface roughness under different treatments were in the ascending order: D_{CK} (1.75 m) < D_{AB} (1.81 m)

Table 1: Fitting SM with its eigenvalues of DEMS

| Rainfall intensity (mm h^{-1}) | Slope | Tillage treatment | SM model | Residual sum of squares | Determination coefficient | Kriging cross validations r^2 (%) |
|---|-------|-------------------|-------------|-------------------------|---------------------------|-------------------------------------|
| 60 | 5° | AB | Spherical | 1.79×10^{-7} | 0.770 | 93.4 |
| | | AD | Gaussian | 1.63×10^{-6} | 0.570 | 95.4 |
| | | CT | Gaussian | 2.66×10^{-7} | 0.300 | 89.5 |
| | | CK | Exponential | 5.73×10^{-10} | 0.440 | 86.3 |
| | 10° | AB | Gaussian | 1.66×10^{-7} | 0.702 | 70.2 |
| | | AD | Linear | 5.36×10^{-6} | 0.383 | 66.2 |
| | | CT | Gaussian | 1.56×10^{-6} | 0.579 | 78.4 |
| | | CK | Exponential | 2.12×10^{-10} | 0.536 | 51.9 |
| | 20° | AB | Spherical | 2.75×10^{-8} | 0.611 | 79.2 |
| | | AD | Spherical | 4.14×10^{-7} | 0.790 | 84.2 |
| | | CT | Gaussian | 2.89×10^{-7} | 0.546 | 86.3 |
| | | CK | Exponential | 2.36×10^{-10} | 0.896 | 55.4 |
| 90 | 5° | AB | Linear | 1.05×10^{-9} | 0.625 | 88.0 |
| | | AD | Gaussian | 1.26×10^{-8} | 0.569 | 86.6 |
| | | CT | Gaussian | 8.50×10^{-8} | 0.458 | 80.6 |
| | | CK | Gaussian | 6.76×10^{-9} | 0.342 | 92.8 |
| | 10° | AB | Gaussian | 2.50×10^{-8} | 0.315 | 93.6 |
| | | AD | Gaussian | 8.84×10^{-8} | 0.647 | 91.4 |
| | | CT | Gaussian | 1.22×10^{-7} | 0.262 | 71.9 |
| | | CK | Linear | 7.38×10^{-10} | 0.382 | 97.8 |
| | 20° | AB | Gaussian | 1.34×10^{-8} | 0.281 | 88.8 |
| | | AD | Gaussian | 1.34×10^{-7} | 0.470 | 69.7 |
| | | CT | Gaussian | 2.88×10^{-8} | 0.453 | 58.1 |
| | | CK | Gaussian | 8.01×10^{-10} | 0.254 | 60.8 |

Note: (1) Data were processed by GS + statistical software. (2) An SM graph might have random or systematic behaviors that can be described by theoretical models (linear, spherical, Gaussian, or exponential). A higher determination coefficient or a smaller residual sum of squares of the theoretical model indicated a better fit and provided a precise test for the advantages and disadvantages of the model. (3) The r^2 is a key indicator used to evaluate goodness-of-fit of the SM model. Normally, the value of $r^2 > 80\%$, $50\text{--}80\%$, $30\text{--}50\%$, or $<30\%$ indicates the correlation between the fitting curve model and the realistic microtopography was strong, medium, weak, or had no relationship, respectively.

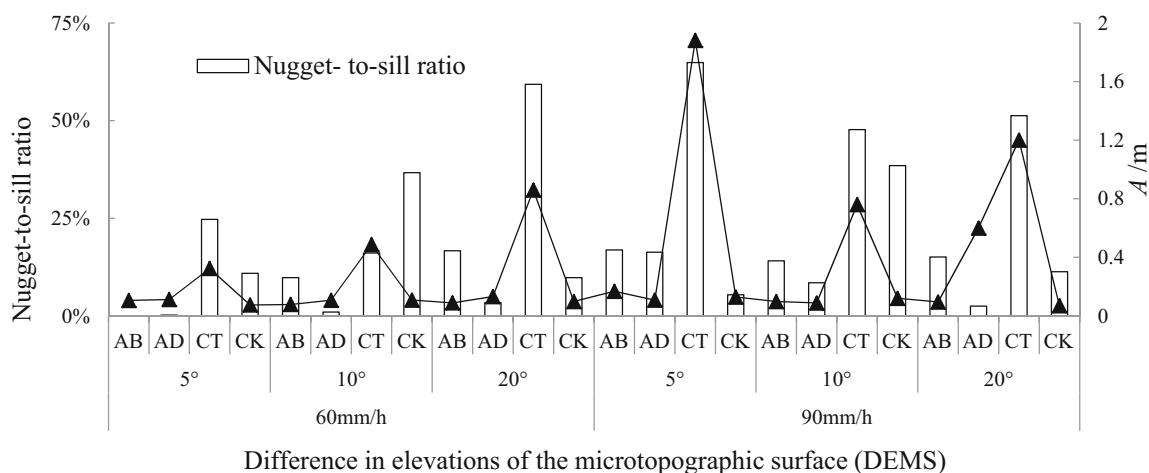


Figure 2: Fitting SM with its parameters of DEMS.

$< D_{AD}$ (1.82 m) $< D_{CT}$ (1.90 m). This indicated that surface CK had the smallest D value. The D value of DEMS treated with CT was the greatest. (3) The D value of

DEMS at rainfall intensities of 60 and 90 mm h^{-1} was 1.75 and 1.88 m, respectively. This result showed an increase in the D value when the rainfall intensity increased.

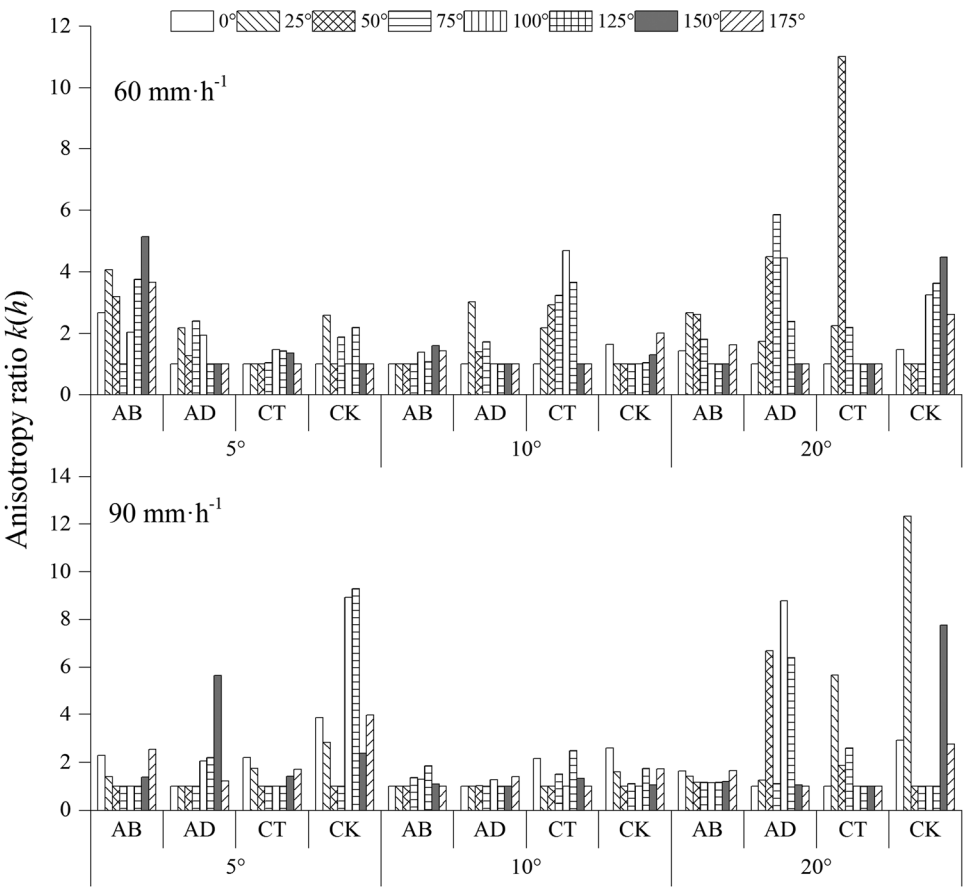


Figure 3: The anisotropy in sheet erosion. The direction of 0° was the longitudinal direction pointing to the top of the microtopographic surface located at the center of left edge of the soil tank.

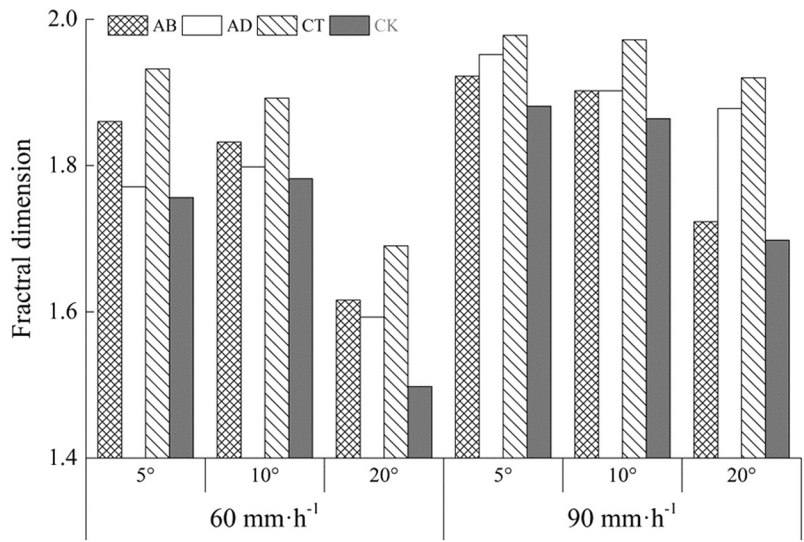


Figure 4: Fractal dimension of DEMS in sheet erosion.

Table 2: Fractal parameters for different types of tillage system, before rainfall, after rainfall, and their difference

| Rainfall intensity (mm h ⁻¹) | Fractal dimension – <i>D</i> | | | | | | | | | Crossover length – <i>l</i> | | | | | | | | |
|--|------------------------------|------|------|------|------|------|------|------|------|-----------------------------|------|------|------|------|------|------|------|------|
| | 5° | | | 10° | | | 20° | | | 5° | | | 10° | | | 20° | | |
| | BE | AE | DI | BE | AE | DI | BE | AE | DI | BE | AE | DI | BE | AE | DI | BE | AE | DI |
| AB | | | | | | | | | | | | | | | | | | |
| 60 | 1.63 | 1.67 | 1.86 | 1.80 | 1.75 | 1.83 | 1.81 | 1.81 | 1.62 | 1.73 | 1.67 | 1.07 | 1.44 | 2.30 | 1.07 | 2.34 | 2.22 | 1.08 |
| 90 | 1.86 | 1.84 | 1.92 | 1.78 | 1.79 | 1.90 | 1.82 | 1.78 | 1.72 | 1.47 | 3.07 | 1.03 | 1.41 | 1.38 | 1.04 | 1.06 | 1.19 | 1.05 |
| AD | | | | | | | | | | | | | | | | | | |
| 60 | 1.76 | 1.77 | 1.77 | 1.78 | 1.79 | 1.80 | 1.81 | 1.78 | 1.59 | 1.09 | 1.19 | 1.09 | 1.09 | 1.07 | 1.07 | 1.54 | 1.55 | 1.12 |
| 90 | 1.79 | 1.81 | 1.95 | 1.79 | 1.78 | 1.90 | 1.79 | 1.79 | 1.88 | 1.06 | 1.54 | 1.06 | 1.55 | 1.09 | 1.05 | 1.55 | 1.07 | 2.89 |
| CK | | | | | | | | | | | | | | | | | | |
| 60 | 1.69 | 1.73 | 1.76 | 1.73 | 1.63 | 1.78 | 1.87 | 1.83 | 1.50 | 2.20 | 2.01 | 1.07 | 1.20 | 1.92 | 2.28 | 1.09 | 1.26 | 2.39 |
| 90 | 1.72 | 1.73 | 1.88 | 1.69 | 1.72 | 1.86 | 1.53 | 1.50 | 1.70 | 1.32 | 1.55 | 1.08 | 1.63 | 1.60 | 1.38 | 1.21 | 1.21 | 1.05 |
| CT | | | | | | | | | | | | | | | | | | |
| 60 | 1.82 | 1.82 | 1.93 | 1.74 | 1.77 | 1.89 | 1.82 | 1.80 | 1.69 | 1.05 | 1.05 | 1.04 | 2.86 | 1.91 | 1.04 | 1.04 | 1.05 | 1.05 |
| 90 | 1.77 | 1.75 | 1.98 | 1.81 | 1.82 | 1.97 | 1.80 | 1.79 | 1.92 | 2.45 | 1.28 | 2.60 | 1.04 | 1.28 | 1.13 | 1.05 | 1.27 | 1.04 |

BE, before rainfall; AE, after rainfall; DI, difference. AB, artificial backhoe; AD, artificial digging; CT, contour tillage; CK, linear slope.

In summary, DEMS treated with CT has the weakest effect on spatial autocorrelation, stronger effect on anisotropy, and resulted in complex spatial distribution of microtopographic features. Therefore, DEMS treated with CT has strong influence on spatial variability.

To better illustrate the relationship between geostatistical indices and two fractal parameters, *D* and *l*, fractal parameters for surface roughness, and their differences in elevation are listed in Table 2. It is apparent from the results in Table 2 that the variability of the fractal dimension was rather homogeneous for all the classes, but the crossover length, *l*, behaved completely differently, although they were relatively close. Changes in average fractal dimension, *D*, induced by 1.78 ± 0.09 , were relatively small, when compared with the change in crossover length, *l* (1.44 ± 0.53). Thus, crossover length was a much more sensitive parameter than fractal dimension to describe soil surface evolution, which is also in accordance with literature results [25,27–29].

3.2 Dynamics between surface microtopography and sheet erosion

3.2.1 Change in surface elevation

At different rainfall intensities, the ratios between changes in elevation of surfaces AB, AD, and CT were negative, while the ratio for surface CK was positive

(Figure 5). These results showed that there was an increase in elevation at the lower half of the soil surface during the sheet erosion process.

When rainfall intensity shifted from 60 to 90 mm h⁻¹, the mean elevation change rate increased from 6.5% to 8.4%. Meanwhile, the mean elevation change rate increased from 5.6% to 35.2% and then to 70.7% as the slope gradient shifted from 5° to 10° and then to 20°. This showed that with the increase in rainfall intensity and slope gradient, the sheet erosion became stronger. Additionally, the mean elevation change rate for each tillage treatment was in the descending order of CK > 0 > AB > AD > CT, which indicated that all tillage treatments had smoothing effect on sheet erosion except CK.

3.2.2 Regression analysis of runoff and sediment

In order to investigate the effect of slope gradient on runoff and sediment yield, the logarithmic function was adopted for modeling analysis (Table 3). The mean runoff yield and the mean sediment yield increased, respectively, from 4.68 to 42.91 kg min⁻¹ and from 367.27 to 449.70 g min⁻¹ with the rainfall intensity changing from 60 to 90 mm h⁻¹. The runoff yield or the sediment yield would increase at a bigger slope gradient. Accordingly, the surface CT has the least runoff and sediment yield (0.57 kg min⁻¹ and 45.35 g min⁻¹). These results showed that treatment CT had a stronger effect on reducing runoff and sediment yield during the sheet erosion process.

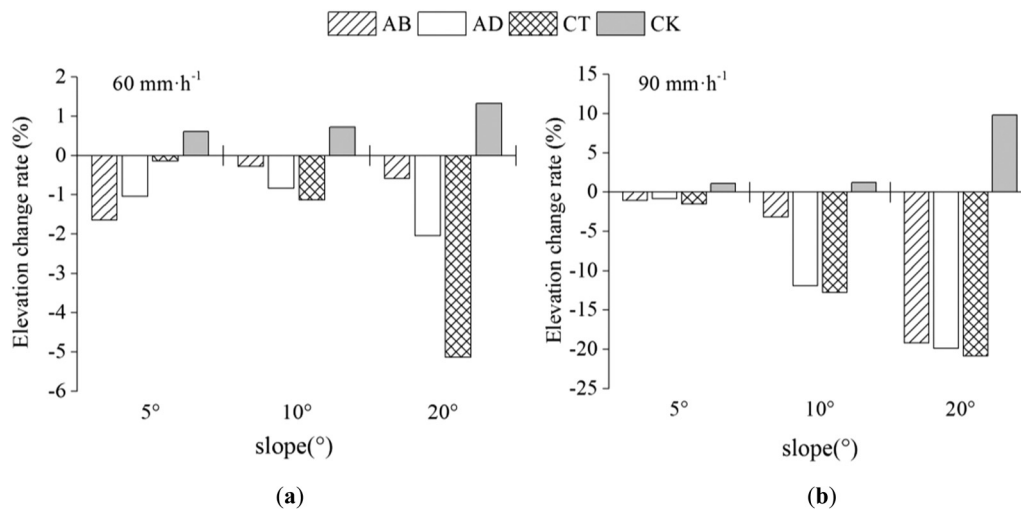


Figure 5: Surface microtopography of elevation change during sheet erosion under rainfall of (a) 60 mm h⁻¹ and (b) 90 mm h⁻¹.

4 Discussion and conclusion

When compared with the previous work of our research group [14,15], the measurement of the runoff and sediment yield was implemented, the specific sheet erosion stage was specially observed instead of a complete erosion development process of before erosion – splash erosion – sheet erosion – rill erosion, the DEMS data were adopted rather than the DEM data, and the effect of rainfall intensity was considered too. At the same time, the SM-based methodological framework [14] integrated with two fractal indices was successfully used to analyze spatial variability of laboratory surfaces at a microtopographic scale. Result of this study confirmed the relevancy of two fractal indices. Fractal dimension D can be taken as a descriptor of horizontal variations of surface microtopography, which describes the distribution of sized structural elements on the soil surface microtopography, whereas crossover length l can be taken as a discriminator of vertical differences in microtopography [24,30]. Horizontal parameter did not show such a clear pattern, and the other one, crossover length l , was more sensitive to rainfall force to describe soil surface evolution.

Most DEMS indices and parameters in the sheet erosion stage showed a strong spatial autocorrelation, a relatively stable spatial structure, a weak randomness, and a spatial dependence that increased with the sampling intervals. The results were exactly consistent with the previous studies.

Combining with previous studies [3,13–15], factors of tillage, slope, and rainfall were proved to have impact on the dynamic spatial variability of the laboratory surfaces

whether in the whole erosion development process or a separate sheet erosion stage. In general, surface CT was mainly affected by the spatial structure, and its spatial variability was greater than surfaces created with other treatments. Therefore, it has a better spatial structure and a soil and water conservation effect to reduce runoff and sediment yield, and the runoff and sediment yield can be described by a logarithmic function of slope. Undoubtedly, agricultural tillage measure of CT can be safely adopted and popularized in the serious soil erosion regions such as the Chinese Loess Plateau.

Surface roughness can be accurately characterized by SM (Gaussian) models. Furthermore, DEMS at the sheet erosion stage has preferable fractal properties with their fractal dimensions ranging from 1.50 to 1.98.

Complexity of surface roughness combined with force of rainfall tended to result in a reduction of spatial variability during the sheet erosion process. Therefore, it can be generalized that rainfall during the sheet erosion stage has a smoothing effect on the soil surface, which is accompanied by a corresponding increase in the complexity of the spatial distribution. The larger the rainfall intensity, the higher the spatial variability, nugget-to-sill ratio, range, anisotropy ratio, fractal dimension, and the mean elevation change rate. So, it is not too much to say that the rainfall intensity in the sheet erosion stage is the main driving factor leading to the change in the spatial distribution of the soil surface.

Moreover, according to our previous works, the mean range (codomain) of slope CT is 1.54 m [31] and 2.0 m [15] at a rainfall intensity of 60 and 90 mm h⁻¹, respectively, when the DEM data were adopted. However, when the DEMS data were adopted, the average

Table 3: Relationship between runoff-sediment yield with slope

| | Tillage | Rainfall density/mm h ⁻¹ | Regression equation | R ² | Sediment yield | Tillage | Rainfall density/mm h ⁻¹ | Regression equation | R ² |
|--------------------|---------|-------------------------------------|----------------------------|----------------|----------------------|---------|-------------------------------------|------------------------------|----------------|
| Runoff yield | AB | 60 | $v = 2.02 \ln(s) - 3.47$ | 0.79 | Sediment yield | AB | 60 | $y = 114.67 \ln(s) - 178.57$ | 0.73 |
| | | 90 | $v = -4.41 \ln(s) + 13.6$ | 0.66 | | | 90 | $y = 109.02 \ln(s) - 124.35$ | 0.94 |
| | AD | 60 | $v = 1.41 \ln(s) - 2.47$ | 0.79 | | AD | 60 | $y = 75.66 \ln(s) - 91.26$ | 0.65 |
| | | 90 | $v = 0.20 \ln(s) + 0.127$ | 0.54 | | | 90 | $y = 18.49 \ln(s) + 6.97$ | 0.75 |
| Total runoff yield | CT | 60 | $v = 0.89 \ln(s) - 1.57$ | 0.79 | Total sediment yield | CT | 60 | $y = 57.04 \ln(s) - 76.25$ | 0.84 |
| | | 90 | $v = -4.41 \ln(s) + 13.6$ | 0.66 | | | 90 | $y = 17.70 \ln(s) - 5.13$ | 0.84 |
| | CK | 60 | $v = 2.76 \ln(s) - 4.13$ | 0.66 | | CK | 60 | $y = 175.01 \ln(s) - 259.20$ | 0.74 |
| | | 90 | $v = 38.39 \ln(s) - 54.16$ | 0.89 | | | 90 | $y = 184.17 \ln(s) - 186.21$ | 0.81 |
| Total runoff yield | | 60 | $v = 7.09 \ln(s) - 11.64$ | 0.73 | | | 60 | $y = 422.37 \ln(s) - 605.28$ | 0.73 |
| | | 90 | $v = 33.28 \ln(s) - 33.73$ | 0.96 | | | 90 | $y = 29.38 \ln(s) - 308.71$ | 0.96 |

Note: The general equation is given by $a = b \ln(s) + c$ ($R^2 > 0.5$), where a is the runoff yield v (kg/mm), b and c are coefficient regressions; s is the slope ($^\circ$). AB, artificial backhoe; AD, artificial digging; CT, contour tillage; CK, linear slope.

range increased from 0.23 to 0.39 m when the rainfall intensity increased from 60 to 90 mm h⁻¹. Thus, the DEMS data are more precise to reflect the difference in elevations and the range or scale (minimum suitable length) for the spatial heterogeneity research.

Slope gradient is one of the critically important factors that drive the erosional response of microtopographic surfaces through the gradual filling of depressions. By comparison of CK with other three treatments, a steeper slope could offset the effect of rainfall in sheet erosion. However, whether a critical slope exists for appropriate tillage still needs further study.

The change in elevations of microtopographic surfaces during rainfall erosion is a critically complex geomorphological and hydrological process. Knowing the impact of rainfall and slope on the runoff and sediment and then quantifying these two parameters have a great significance for developing a more precise erosion model at a microtopographic scale.

Acknowledgments: This study was supported by the National Natural Science Foundation of China (Grant No. 41371273 and 41701239). The authors would like to thank the editors and anonymous reviewers for their valuable comments and suggestions, which greatly improved this work.

Author contributions: The authors applied the SDC approach for the sequence of authors. ZQF designed the experiments and TN carried them out. TN, ZCT and DHR performed the model calibrations and simulations. TN and ZCT prepared the original manuscript with contributions from all co-authors. TN and ZCT contributed equally to this work and should be considered co-first authors.

Conflict of interest: The authors declare no conflict of interest.

References

- [1] Borrelli P, Märker M, Schütt B. Modelling post-tree-harvesting soil erosion and sediment deposition potential in the turano river basin (italian central apennine). *Land Degrad Dev.* 2015;26:356–66.
- [2] Berendse F, van Ruijven J, Jongejans E, Keesstra S. Loss of plant species diversity reduces soil erosion resistance. *Ecosystems.* 2015;18:881–8.
- [3] Zhang QF, Zhao LS, Wang J, Wu FQ. Spatiotemporal variability and simulation of tillaged loess microtopography in water erosion. *J Soil Water Conservat.* 2014;69:343–51.
- [4] Liu JE, Wang ZL, Gao SJ, Zhang KD. Experimental study on hydrodynamic mechanism of sheet erosion processes on loess hillslope. *Trans Chinese Soc Agric Eng.* 2012;28:144–9.

- [5] Palmer RS. The influence of a thin water layer on waterdrop impact forces. *Int Assoc Sci Hydrol Publ.* 1963;65:141–8.
- [6] Chu XF, Nelis J, Rediske R. Preliminary study on the effects of surface microtopography on tracer transport in a coupled overland and unsaturated flow system. *J Hydrol Eng.* 2013;18:1241–49.
- [7] El Kateb H, Zhang HF, Zhang PC, Mosandl R. Soil erosion and surface runoff on different vegetation covers and slope gradients: a field experiment in southern shaanxi province, china. *Catena.* 2013;105:1–10.
- [8] Komatsu Y, Kato H, Zhu B, Wang T, Yang F, Rakwal R, et al. Effects of slope gradient on runoff from bare-fallow purple soil in china under natural rainfall conditions. *J Mount Sci.* 2018;15:738–51.
- [9] Tapia-Vargas M, Tiscareño-López M, Stone JJ, Oropeza-Mota JL, Velázquez-Valle M. Tillage system effects on runoff and sediment yield in hillslope agriculture. *Field Crops Res.* 2001;69:173–82.
- [10] Dutilleul P. *Spatio-temporal heterogeneity: concepts and analyses.* New York, NY, USA: Cambridge University Press; 2011.
- [11] Wang JF, Zhang TL, Fu BJ. A measure of spatial stratified heterogeneity. *Ecol Indic.* 2016;67:250–6.
- [12] Robson BA, Nuth C, Nielsen PR, Girod L, Hendrickx M, Dahl SO. Spatial variability in patterns of glacier change across the manaslu range, Central Himalaya. *Front Earth Sci.* 2018;6:12.
- [13] Zhang HH, Ta N, Zhang QF. Spatial heterogeneity of loess contour tilled microtopographic slope in rainfall erosion. *Soil Sci Plant Nutr.* 2016;62:409–15.
- [14] Zhang QF, Wang J, Wu FQ. Spatial heterogeneity of surface roughness on tilled loess slopes in erosion stages. *Soil Water Res.* 2018;13:90–7.
- [15] Zhang QF, Wang J, Zhao LS, Wu FQ, Zhang ZY, Torbert AH. Spatial heterogeneity of surface roughness during different erosive stages of tilled loess slopes under a rainfall intensity of 1.5 mm min⁻¹. *Soil Till Res.* 2015;153:95–103.
- [16] WRB, I.W.G. World reference base for soil resources 2014: International soil classification system for naming soils and creating legends for soil maps. *World Soil Resources Report* 2014, No. 106. FAO, Rome.
- [17] An J, Zheng FL, Lu J, Li GF. Investigating the role of raindrop impact on hydrodynamic mechanism of soil erosion under simulated rainfall conditions. *Soil Sci.* 2012;177:517–26.
- [18] Zheng FL, Zhao J. A brief introduction on the rainfall simulation laboratory and equipment. *Res Soil Water Conserv.* 2004;11:177–8.
- [19] Shen HO, Zheng FL, Wen LL, Lu J, Jiang YL. An experimental study of rill erosion and morphology. *Geomorphology.* 2015;231:193–201.
- [20] Zhao LS, Zhang QF, Liang XL, Cao WP, Wu FQ. Establishment and application of dem for loess slope land based on gis. *Trans Chinese Soc Agric Eng.* 2010;26:317–22.
- [21] Ta N, Wang J, Zhang HH, Tian L, Zhang QF. Variation characteristics of micro-topography in tillage loess slope during splash erosion. *Bull Soil Water Conserv.* 2016;36:110–4.
- [22] Pandey V, Pandey PK. Spatial and temporal variability of soil moisture. *International J Geosci.* 2010;1:87–98.
- [23] Al-Karni AA, Al-Shamrani MA. Study of the effect of soil anisotropy on slope stability using method of slices. *Comput Geotech.* 2000;26:83–103.
- [24] Vázquez EV, Vieira SR, De Maria IC, González AP. Fractal dimension and geostatistical parameters for soil microrelief as a function of cumulative precipitation. *Sci Agric.* 2010;67:78–83.
- [25] Vázquez EV, Miranda JGV, González AP. Characterizing anisotropy and heterogeneity of soil surface microtopography using fractal models. *Ecol Modell.* 2005;182:337–53.
- [26] Jia XH, Li XR, Zhang JG, Zhang ZS. Analysis of spatial variability of the fractal dimension of soil particle size in *ammodendron mongolicum* desert habitat. *Environ Geol.* 2009;58:953–62.
- [27] Martínez-Agirre A, Álvarez-Mozos J, Giménez R. Evaluation of surface roughness parameters in agricultural soils with different tillage conditions using a laser profile meter. *Soil Till Res.* 2016;161:19–30.
- [28] Huang CH, Bradford JM. Applications of a laser scanner to quantify soil microtopography. *Soil Sci. Soc Am J.* 1992;56:14–21.
- [29] Eltz FLF, Norton LD. Surface roughness changes as affected by rainfall erosivity, tillage, and canopy cover. *Soil Sci Soc Am J.* 1997;61:1746–55.
- [30] Huang CH. Quantification of soil microtopography and surface roughness. In: Baveye P, Parlange JY, Stewart BA, editors. *Revival: fractals in soil science.* Boca Raton, FL, USA: CRC Press; 1998. p. 153–68.
- [31] Zhang L, Zhang QF, Zhao LS, et al. Spatial heterogeneity of loess tilled slope surface roughness. *Sci Agric Sin.* 2014;47:2363–74.